Development of a Long-Acting Insulin Analog Using Albumin Fusion Technology

Alokesh Duttaroy, Palanisamy Kanakaraj, Blaire L. Osborn, Helmut Schneider, Oxana K. Pickeral, Cecil Chen, Guiyi Zhang, Shashi Kaithamana, Mallika Singh, Robert Schulingkamp, Dan Crossan, Jason Bock, Thomas E. Kaufman, Peter Reavey, Melisa Carey-Barber, Surekha R. Krishnan, Andy Garcia, Kelly Murphy, Jana K. Siskind, Malia A. McLean, Susan Cheng, Steve Ruben, Charles E. Birse, and Olivier Blondel

The primary therapeutic goal for the treatment of diabetes is maintenance of a long-term, near-normoglycemic condition and prevention of the onset or progression of the complications associated with the disease. Although several analogs of human insulin have been developed, the currently prescribed long-acting insulin analogs do not provide a stable basal glycemia for more than a few hours. Here, we report the development of Albulin, a long-acting insulin analog obtained by direct gene fusion of a single-chain human insulin to human serum albumin. Albulin showed an elimination $t_{1/2}$ of ~7 h in normoglycemic mice. In vitro pharmacodynamic profiles for Albulin characterized by receptor binding, inhibition of gluconeogenesis, induction of glucose uptake, and global regulation of gene expression in relevant cell types showed that Albulin produced similar activity profiles compared with that of recombinant human insulin. A single Albulin administration in vivo normalized blood glucose level in diabetic mice in a relatively peakless and sustained (24-h) fashion. A further reduction in glucose levels was achieved by administering a recombinant human insulin a few hours after Albulin injection in mice, indicating the potential for Albulin therapy in combination with available fast-acting insulin derivatives. In summary, Albulin displays characteristics of a potent long-acting insulin analog that can be evaluated for use as a novel insulin therapy for patients with insulin-dependent diabetes. *Diabetes* 54:251–258, 2005

Management of type 1 and type 2 diabetes with insulin therapy typically includes a long-acting basal component for between-meal and nocturnal glycemic control, together with preprandial bolus injections of a short-acting insulin for control of meal-stimulated increases in glucose levels (1,2). Molecular genetics has opened new opportunities to create insulin analogs by changing the structure of the native protein to improve its therapeutic properties (3,4). Various strategies, including elongation of the COOH-terminal end of the insulin B-chain (insulin glargine [5,6]) and engineering of fatty acid–acylated insulins with substantial affinity for albumin (insulin detemir [7]), are being used to develop long-acting insulin analogs. However, in vivo treatments with available long-acting insulin analogs still result in a high frequency of hypo- and hyperglycemic excursions (8) and modest reduction in HbA_{1c} (9). Development of a truly long-acting and stable human insulin analog still remains an important task (10).

It is possible to obtain more stable forms of a circulating protein using gene fusion technology between the coding sequences for the protein of interest and for human serum albumin (HSA). Proteins resulting from HSA gene fusions have the long circulating life of albumin while retaining their biological and therapeutic properties (11,12). Here we report the development of Albulin, a biologically active recombinant analog of human insulin fused to HSA, and compare the relative biological activities of Albulin and insulin in vitro and in vivo.

RESEARCH DESIGN AND METHODS

Expression and purification of Albulin. A synthetic gene construct encoding a single-chain insulin containing the B- and A-chain of mature human insulin linked together by a dodecapeptide linker was obtained using four overlapping oligonucleotide primers and PCR amplification. The resulting PCR product was ligated in-frame between the signal peptide of HSA and the NH_2-terminus of mature HSA, contained within a pSAC35 vector for expression in yeast (pSAC35-Albulin). The same synthetic gene was also cloned in-frame between a myeloid progenitor inhibitory factor-1 signal peptide sequence and the NH_2-terminus of HSA into pC4, a mammalian proprietary expression vector (pC4.Albulin). Chinese hamster ovary (CHO) cells were stably transfected with pC4.Albulin with Lipofectamine 2000 (Invitrogen) using the manufacturer's protocol. The Albulin-expressing single clones were selected based on HSA enzyme-linked immunosorbent assay (ELISA). Albulin resulting from expression in yeast or CHO cells was purified using conventional chromatographic methods. Studies reported in this article were performed using Albulin expressed in both yeast and CHO cells.

Receptor binding assays. Competition binding to the human insulin receptor was assayed in a 96-well plate using 0.6×10^6 IM-9 B-cells/well in 100 μl complete medium (RPMI 10% fetal bovine serum) with 0.3 nmol/l ^{125}I-labeled insulin (Amersham; specific activity, 2,000 Ci/mmol) in the absence or presence of various concentrations of unlabeled Albulin or insulin. Competition binding to the IGF-I receptor was assayed in rat L6 myoblasts (2×10^6 cells/well) using 0.3 nmol/l ^{125}I-labeled IGF-I (Amersham; specific activity, 2,000 Ci/mmol). Binding reaction was performed at room temperature for 2 h on a shaker platform. The bound and unbound ligands were separated by centrifugation through 200 μl of 1.5 dibutylphthlate/1.0 bis (2-ethyl-hexyl)

From Human Genome Sciences, Rockville, Maryland.

Address correspondence and reprint requests to Olivier Blondel, Division of Diabetes, Endocrinology and Metabolic Diseases, NIDDK/NIH, 6707 Democracy Blvd., Rm. 606, MSC5460, Bethesda, MD 20892-5460. E-mail: olivier.blondel@verizon.net.

Received for publication 12 February 2004 and accepted in revised form 11 October 2004.

DMEM, Dulbecco's modified Eagle's medium; ELISA, enzyme-linked immunosorbent assay; FAS, fatty acid synthase; HSA, human serum albumin; SEAP, secreted embryonic alkaline phosphatase; SREBP, sterol regulatory element-binding protein; STZ, streptozotocin.

phthalate mixture in a polyethylene microfuge tube (Bio-Rad, Hercules, CA) for 20 s. The cell pellet in the bottom of the tube containing the bound radiolabeled ligand was cut off using a tube cutter and counted in a γ counter. Binding data were analyzed by Prism (GraphPad Software, San Diego, CA) to determine the concentration that results in 50% inhibition (IC_{50}) values.

Proliferation assays. Proliferation assays were performed using rat H9C2 cardiomyoblasts and rat L6 myoblasts. A total number of 1×10^4 cells/well were plated in a 96-well plate and starved for 24 h in serum-free medium. Cells were treated with various concentrations of insulin or Albulin in 100 μl RPMI medium containing 0.5% fetal bovine serum for 24 h at 37°C. ^{3}H-thymidine (5 μCi) was added to each well, and cells were incubated for another 6 h. Cells were harvested, and ^{3}H-thymidine incorporation was measured on a scintillation counter.

Glucose uptake assay in 3T3-L1 adipocytes. Murine 3T3-L1 fibroblasts were grown and differentiated into adipocytes as previously described (13). A modification of a method (14) was used for the measurements of 2-deoxyglucose uptake. A 96-well plate containing 3T3-L1 adipocytes was washed twice with Dulbecco's modified Eagle's medium (DMEM) low glucose (Life Technologies). Insulin and Albulin were added for 30 min, followed by addition of 0.1 mmol/l 2-deoxy-D-[2,6^3-H]glucose (0.5 mCi/mmol) for 10 min at 37°C.

Glucose production assay. A previously described protocol (15) was adapted for a 96-well format. H4IIE cells were grown in high-glucose DMEM containing 10% fetal bovine serum in a humidified incubator at 37°C and 5% CO_2 and assayed after reaching 90% confluency. Dilution series of growth/differentiation factor 2 and bovine insulin were prepared in serum-free DMEM (high glucose) containing 500 μg/ml bovine serum albumin, and 100 μl was added to the 60 inner wells (six wells per data point were used). The plates were incubated for 17 h at 37°C. The cells were then washed three times with 200 μl Dulbecco's PBS. Glucose production media consisting of glucose-free DMEM containing 40 mmol/l sodium DL-lactate and 2 mmol/l sodium pyruvate were added to the wells (100 μl), and incubation was continued for 5 h at 37°C. The supernatant was then harvested, and the cells were lysed in 200 μl 1% (wt/vol) sodium dodecyl sulfate in PBS. Glucose concentrations were measured using the Amplex Red kit (#A22177) from Molecular Probes (Eugene, OR). Glucose concentrations were calculated using Prism software and adjusted for protein concentrations.

Reporter assays. The *PEPCK* (*PEPCK-SEAP* [secreted embryonic alkaline phosphatase]) reporter construct was based on the promoterless pSEAP2-neo vector that contained the wild-type *PEPCK* promoter sequence from −600 to +69 fused to the *SEAP* gene. Stable *H4IIe/PEPCK-SEAP* reporter cells were treated with 0.5 μmol/l dexamethasone for 18 h to activate the *PEPCK* promoter before addition of Albulin or insulin. After a 48-h incubation period, conditioned media were removed, and SEAP activity was determined using the manufacturer's recommended protocol (Tropix Phospha-Light System, Applied Biosystems, Bedford, MA).

In similar experiments, promoter regions for human *malic enzyme* (bp: −1,183 to −77) and *fatty acid synthase* (*FAS*) (bp: −444 to +8), as well as the sterol regulatory element-binding protein (SREBP) binding element from the human *FAS* promoter (GGGGTACCTCATTGGCCTGGGCGGCGCAGCCAAGC TGTCAGCCCATGTGGCGTGGCCGCCCCTCGAGCGG), were cloned into pSEAP2-neo. The constructs were transfected into H4IIe cells, and stable clones were selected. Cells were serum deprived for 18–24 h before being treated with Albulin or insulin. After a 48-h incubation, conditioned medium was harvested and SEAP activity was measured.

cDNA microarrays. The effect of treatment on gene expression was assayed using cDNA array hybridization technology as previously described (12). In these experiments, human primary adipocytes (ZenBio) were starved overnight in low glucose media (DMEM), before treatment with insulin or Albulin at a concentration corresponding to the half-maximal concentration (EC_{50}) and 10× EC_{50} as determined using the glucose uptake assay described above. RNA was isolated in TRIZOL after 2 or 6 h of treatment. ^{33}P-labeled cDNA probes were synthesized from 3 μg total RNA, hybridized to cDNA arrays overnight, and washed under stringent conditions. Hybridization signal was detected after 4 days using a FUJI BAS 2500 phosphorimaging system. The signal from duplicate spots representing particular genes was captured and quantitated using ImaGene 4.0 software (BioDiscovery). cDNA array results were confirmed for a subset of genes using a one-step 25-μl quantitative RT-PCR (qPCR) using 50 ng mRNA. The relative abundance of specific mRNAs were normalized to 18S rRNA using the Applied Biosystems Prism 7700 sequence detection system. Primer and probe sets were obtained from Applied Biosystems to target the following human sequences (accession numbers are given in parentheses): *DEPP* (NM_007021), *ID3* (NM_002167), *ADM* (NM_001124), *CRABP2* (NM_001878), and 18S rRNA (M10098).

In vivo effect of Albulin on glycemia. All mice (male, Balb/cJ, 11 weeks old, 20–25 g, purchased from Taconic) were housed in the Human Genome Sciences animal facility area (12-h day:12-h night cycle) and were provided with regular food and water ad libitum. All animal studies were conducted according to the Human Genome Sciences guidelines for standard animal care and usage. Blood glucose levels were measured via the tail vein using a OneTouch Ultra Glucometer (LifeScan) in all experiments. Mice were rendered diabetic after a single intravenous administration of streptozotocin (STZ) (175 mg/kg; Sigma; freshly formulated in 0.9% NaCl). Mice were then allowed to recover for 4 days. Blood glucose levels were measured to assure hyperglycemia in freely fed mice. Mice were then injected once subcutaneously with several doses of Albulin (1.0, 2.5, 5.0, and 10.0 mg/kg). Control mice were injected subcutaneously with either vehicle (buffer: 20 nm citrate phosphate, 150 nm NaCl; pH 6.0) or HSA (10.0 mg/kg). Blood glucose levels were measured 1 h before injection, then just before injection time, and then 1, 3, 6, 12, 24, and 36 h after injection.

In the next study, the combined effect of Albulin and Humulin R on blood glucose levels was evaluated in STZ-induced diabetic Balb/cJ mice. Mice were divided into four groups that received either a subcutaneous injection of HSA (2.3 mg/kg), vehicle (buffer), or (remaining two groups) Albulin (2.5 mg/kg). Six hours later, mice that received HSA were injected with vehicle, and vehicle-injected mice were administered with Humulin R (5.0 units/kg). The remaining two Albulin-treated groups were reinjected with either vehicle or Humulin R (5.0 units/kg), yielding four groups: HSA + vehicle (controls), vehicle + Humulin R, Albulin + vehicle, and Albulin + Humulin R (HSA, Albulin, and Humulin R were dosed at an equimolar basis). After the second injection, mice were screened for blood glucose at 15 min, 30 min, and 1, 3, 6, 12, 18, and 30 h.

Finally, the effect of Albulin together with Humulin R was measured in glucose-challenged mice. Four groups of STZ-induced diabetic Balb/cJ mice were fasted overnight and injected subcutaneously with HSA (2.3 mg/kg), vehicle (buffer), or (remaining two groups) Albulin (2.5 mg/kg). Three hours after treatment, mice were injected subcutaneously with either Humulin R (5 units/kg) or vehicle, yielding four groups: HSA + vehicle (controls), vehicle + Humulin R, Albulin + vehicle, and Albulin + Humulin R. Immediately after the second injection, mice were given glucose (1.2 g/kg) orally and screened for blood glucose levels at 15 min, 30 min, and 1, 1.5, 2, 3, 6, and 9 h after the glucose challenge.

Pharmacokinetic studies. Male C57Bl/6 mice (9–10 weeks old, 22–28 g; purchased from The Jackson Laboratories) were injected intravenously (lateral tail vein) or subcutaneously (midscapular region) with 1.0 mg/kg Albulin. Two mice per time point were killed by CO_2 asphyxiation before dosing, at 5 min (intravenous only), 0.5 h (subcutaneous only), and at 1, 2, 6, 24, 48, and 72 h after dosing. Blood was collected from the inferior vena cava, and plasma was analyzed using a sandwich-type ELISA. In this assay, a mouse anti-insulin monoclonal antibody (1 g/ml in $NaHCO_3$) was coated onto a 96-well ELISA plate. Nonspecific sites were blocked with 1% ovalbumin. Diluted plasma samples and standards were incubated on the plate for 2 h. After washing, a biotinylated goat anti-HSA polyclonal antibody was added to detect the Albulin. The signal was generated using a 3,3′,5,5′ tetramethylbenzidine substrate. The reaction was stopped with 50 μl of 1 mol/l H_2SO_4. The OD_{450} was measured, and a standard curve was generated using Softmax software (Molecular Devices). Control studies have indicated that recombinant insulin does not interfere with the measurement of known concentrations of Albulin using this assay. Pharmacokinetic analyses were conducted by compartmental methods (WinNonlin, Version 3.3; Pharsight). The observed individual plasma concentrations at each time point were fit to a one-compartment open model. The intravenous data were analyzed using bolus input and first order output, whereas the subcutaneous data were analyzed using first order input and first order elimination. Data were weighted as $1/C_{pred}^2$ [square of predicted concentration] for analyses of the intravenous and subcutaneous data.

Statistical analysis. Data from all in vivo studies using mice were analyzed by using a one-way repeated-measures ANOVA model with a subsequent pairwise treatment comparison. When the F test P value was <0.05, the treatment effect was considered significant.

RESULTS

Expression and purification of Albulin. Recombinant insulin is traditionally produced by expression of human proinsulin in yeast (16) or *Escherichia coli* (17), followed by endopeptidase-mediated cleavage of C-peptide (18). The posttranslational processing of C-peptide in an insulin-HSA hybrid, however, would likely result in the cleavage of the albumin region. To eliminate the need for posttranslational processing, we have developed Albulin as a single-chain insulin analog that can be produced in

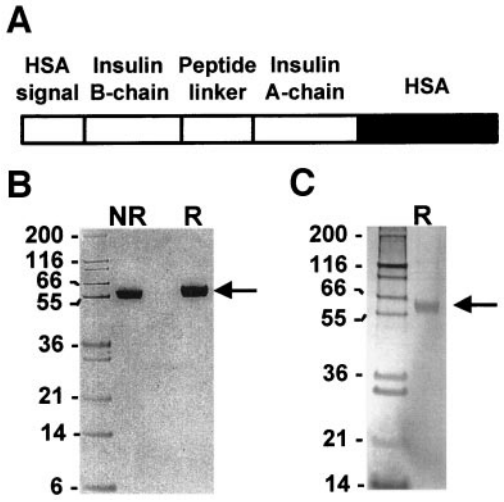

FIG. 1. Structure and purification of Albulin. *A*: Domain structure of the single-chain insulin fused to the NH_2-terminus of recombinant HSA to create Albulin. *B* and *C*: Analysis of Albulin purified from yeast supernatants. A Comassie blue staining of 2.5 μg Albulin after SDS-PAGE analysis in nonreducing (NR) and reducing (R) conditions is shown (*B*). Purified Albulin was resolved by SDS-PAGE and immunoblotted with mAb against human serum insulin (*C*).

yeast or in mammalian cells. Albulin consists of the B- and A-chain of human insulin (100% identity to native human insulin), linked together by a dodecapeptide linker and fused to the NH_2-terminus of the native HSA (Fig. 1*A*). Albulin was collected from yeast supernatants at a concentration of 2–10 mg/l and purified to near 100% homogeneity. Western blotting using a monoclonal antibody raised against human proinsulin resulted in a strong signal with purified Albulin (Fig. 1*C*). NH_2-terminal sequencing confirmed that the Albulin secreted from yeast or CHO cells was formed by the cleavage of the HSA signal peptide and started with the first eight amino acids of the human insulin B-chain (Phe-Val-Asn-Gln-His-Leu-Cys-Gly).

TABLE 1
Potencies of Albulin and insulin in various in vitro assays

	Estimated IC_{50} or EC_{50} (nmol/l)	
	Insulin	Albulin
Binding to insulin receptor	1.1	7.4
Binding to IGF-I receptor	11.7	38.7
Insulin/Albulin-mediated proliferation in H8C2 cells	2.1	2.7
Insulin/Albulin-mediated proliferation in L6 cells	1.40	0.45
Glucose uptake in 3T3-L1 adipocytes	31.4	46.1
Glucose production in H411E hepatocytes	0.51	2.23
SEAP activity in PEPCK reporter assay	2.22	0.25
SEAP activity in SREBP reporter assay	3.30	11.5
SEAP activity in ME reporter assay	18.6	39.8
SEAP activity in FAS reporter assay	39.7	27.1

IC_{50} and EC_{50} values derived from the in vitro pharmacodynamic studies shown in Figs. 2 and 3 are collected in this table to facilitate potency comparisons between the two agents.

Receptor binding and proliferation studies. To characterize the in vitro binding properties of Albulin, competition binding assays were performed in various cell lines that express the insulin receptor (19). Competitive binding data demonstrated that Albulin bound to the insulin receptor in IM-9 cell lines with a binding affinity lower than that of insulin (Fig. 2*A* and Table 1). Similar results were

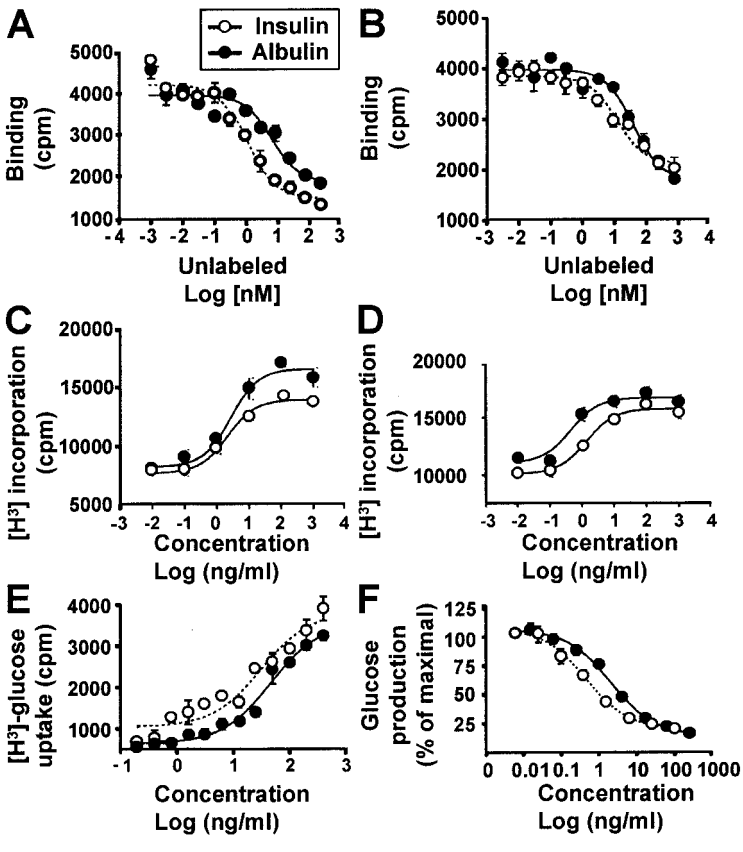

FIG. 2. In vitro properties of Albulin. *A*: Binding to human insulin receptor. IM-9 cells were incubated with 0.1 nmol/l ^{125}I-insulin in the absence or presence of various concentrations of insulin or Albulin. *B*: Binding to the IGF-I receptor. L6 cells were incubated with 0.1 nmol/l ^{125}I–IGF-I in the absence or presence of various concentrations of insulin or Albulin. *C* and *D*: Insulin- and Albulin-induced proliferation in H9C2 (*C*) and L6 (*D*) cells. *E*: Insulin and Albulin effects on glucose uptake in 3T3-L1 adipocytes. *F*: Insulin and Albulin effects on glucose production in H4IIE cells.

obtained using CHO cells overexpressing the human insulin receptor, rat H4IIE hepatoma cells, and human HepG2 hepatoma cells (data not shown).

Insulin can also bind to the IGF-I receptor with a lower affinity than to the insulin receptor (20). To determine the binding affinity of Albulin to the IGF-I receptor, a competition binding assay was performed using ^{125}I-labeled IGF-I in L6 cells. As shown in Fig. 2*B*, Albulin completely displaced ^{125}I–IGF-I, and the binding affinity was slightly lower (threefold) than that of insulin (Table 1).

High affinity for IGF-I receptors of some insulin analogs have been correlated with growth-promoting activity (21). Moreover, certain insulin analogs with higher affinity toward the insulin receptor can produce higher mitogenic responses in vitro (22). To compare Albulin's mitogenic effects to that of insulin, proliferation assays were performed with insulin and Albulin using two commonly used myoblast cells: H9C2 (Fig. 2*C*) and L6 (23) (Fig. 2*D*). Albulin induced proliferation of cells in a dose-dependent fashion showing similar (H9C2) to threefold-higher (L6) potency than that of insulin (Table 1).

In vitro activity of Albulin: glucose uptake and production. Insulin activities include stimulation of peripheral glucose disposal and inhibition of hepatic glucose production (24). The ability of Albulin to mediate these two key biological functions was assayed in vitro, and comparison was made with the activity of recombinant human insulin. First, the effect of insulin and Albulin on glucose uptake in 3T3-L1 adipocytes was investigated. Pretreatment of the cells with insulin or Albulin resulted in a dose-dependent increase in 2-deoxyglucose uptake with very similar characteristics (Fig. 2*E*). Maximal glucose uptake and EC_{50} values (Table 1) were not significantly different between the two proteins. Similar results were obtained using cultured human adipose cells (data not shown). We then examined whether Albulin could regulate the net glucose production in H4IIe hepatoma cells (Fig. 2*F*). Pretreatment of the cells with Albulin led to a dose-dependent inhibition of the amount of glucose released by H4IIe cells in the incubation medium. Albulin was as potent as recombinant human insulin at inhibiting gluconeogenesis in this system (Table 1).

In vitro activity of Albulin: regulation of gene expression. In addition to the direct activation of signaling pathways in target tissues, insulin regulates tissue functions by controlling the transcription of numerous genes involved in growth and metabolism (25). We have used two separate strategies to compare the ability of Albulin and insulin to regulate gene transcription.

The first approach was to evaluate reporter assays using promoter regions of four human genes (e.g., *PEPCK*, *SREBP*, *malic enzyme*, and *FAS*) that are known to be regulated by insulin (Fig. 3). PEPCK is a rate-limiting enzyme in hepatic gluconeogenesis, and the *PEPCK* gene is regulated by insulin (26). Our data showed that treatment of the *PEPCK-SEAP* reporter with either Albulin or insulin strongly inhibited the secretion of SEAP in a dose-dependent manner, and Albulin appeared to be 10 times more potent than insulin (Table 1). Insulin's stimulatory effect on fatty acid synthesis is mediated by SREBP-1c (27). Treatment of the *SREBP-SEAP* reporter with either Albulin or insulin indicates that both Albulin and insulin can induce binding of SREBPs to their cognate sequence with approximately similar efficiency (Table 1). We also tested the effect of Albulin and insulin on the transcription of two other key enzymes involved in hepatic fatty acid metabolism: malic enzyme and FAS (28). Treatment of *FAS* and *malic enzyme* reporters with Albulin or insulin strongly stimulated the secretion of SEAP in a dose-dependent and comparable manner.

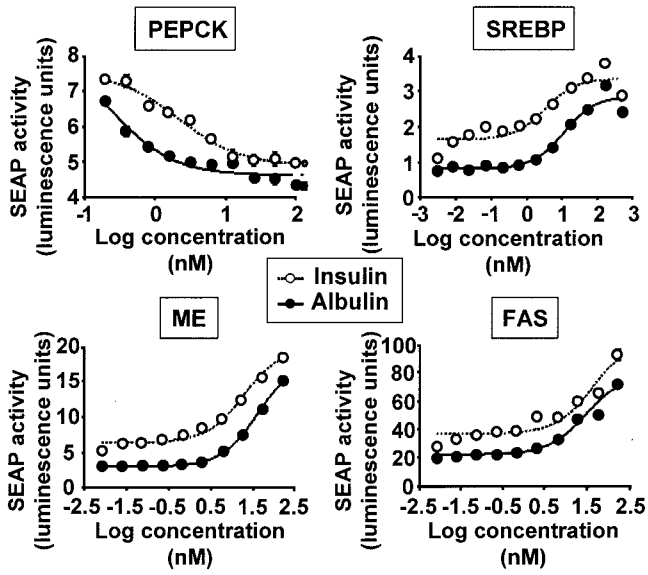

FIG. 3. Comparison of in vitro activities of Albulin and insulin in *PEPCK*-, *SREBP*-, *malic enzyme* (ME)-, and *FAS-SEAP* reporters in H4IIe rat hepatoma cells. Serum-deprived reporter cells were treated with purified recombinant Albulin or insulin at various concentrations. SEAP activity in the conditioned media was measured after a 48-h incubation period as described in RESEARCH DESIGN AND METHODS.

The other approach to determine Albulin's ability to regulate gene transcription was based on cDNA microarray profiling using insulin-responsive cells after Albulin or insulin treatment. A wide-ranging comparison of the effects of Albulin and insulin on global gene expression in human primary adipocytes was performed through cDNA array analysis. Of the 6,476 genes represented on the array, 32 were consistently up- or downregulated at least twofold in at least three of the treatment groups (either Albulin or insulin) compared with the respective control. These 32 genes were organized using unsupervised hierarchical clustering (29) (Fig. 4). Changes in gene expression after treatment with insulin and Albulin were very similar, and no genes were identified that were regulated exclusively by either ligand. The striking similarity of responses to Albulin and insulin is illustrated in the dendrogram arrangement of treatments at 6 h, where responses to the two ligands were found to be more similar than the effects of treating with the same molecule at different concentrations (1× and 10×). The expression profiles observed in the cDNA array analysis were confirmed for a subset of four genes with distinctive regulation patterns (*DEPP*, *ID3*, *ADM*, and *CRABP2*) through qPCR (Fig. 5).

In vivo control of glycemia. The ability of Albulin to reduce hyperglycemia was tested in STZ-induced diabetic mice. A single subcutaneous injection of Albulin in freely fed diabetic mice produced a gradual decline in blood glucose level, with the lowest levels recorded at 6 h postinjection (Fig. 6*A*). The reduction in blood glucose

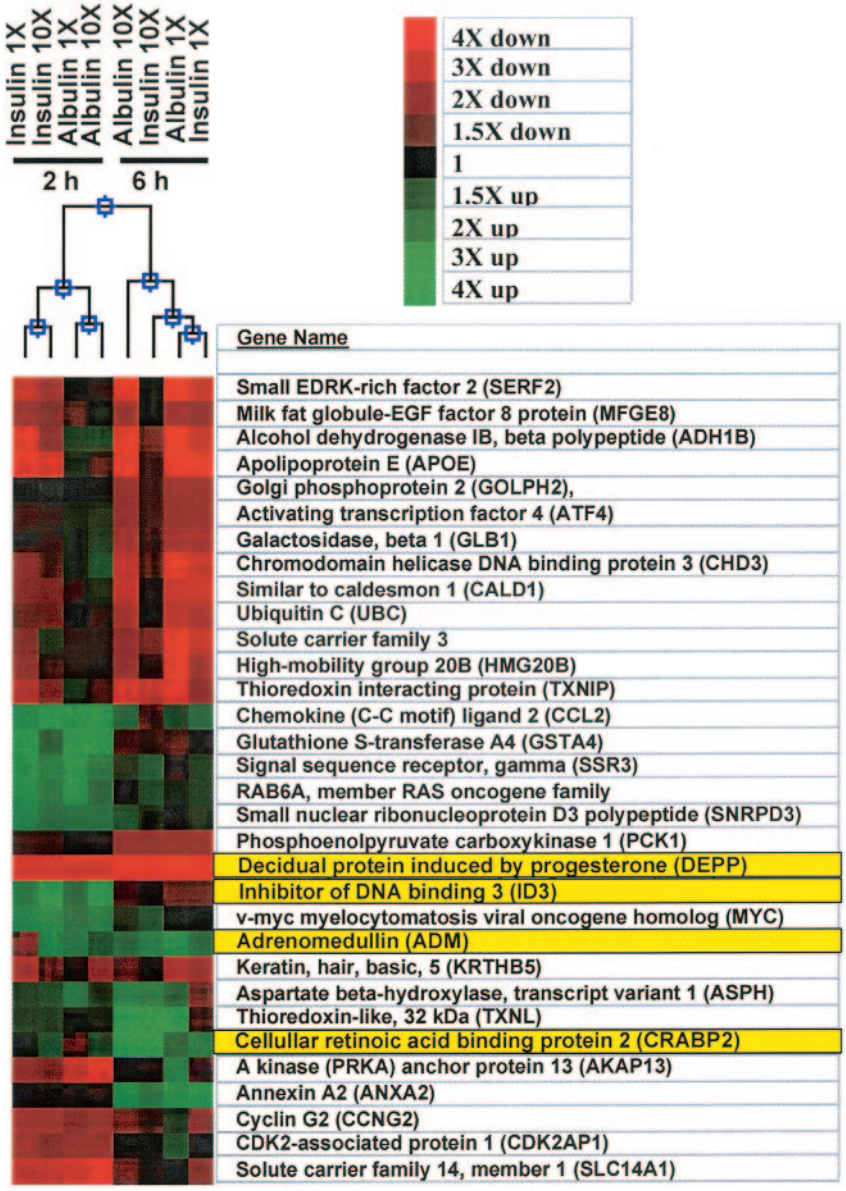

FIG. 4. Global comparison of transcriptional effects of Albulin and insulin. Gene expression profile of adipocytes treated with different concentrations (1× and 10×) of Albulin or insulin for 2 or 6 h. Differential gene expression is shown in pseudocolor as a ratio relative to untreated cells at the appropriate time point (green represents upregulation and red represents downregulation relative to the untreated sample). Each column corresponds to one experimental condition and each row to a unique gene after averaging the normalized values for all duplicate points on the array. The dendrogram illustrates the overall extent of differences in gene expression profiles resulting from alternate treatments. Data points with a coefficient of variation >0.8 between duplicate spots were considered missing.

levels induced by Albulin was relatively slow (peakless), and glycemia remained significantly ($P < 0.05$) lower than control values in vehicle-treated mice for up to 24 h. There was no significant difference between HSA- and vehicle-treated control mice. When compared with HSA control mice, the highest dose of Albulin (10 mg/kg) showed a significant ($P < 0.01$) reduction in glycemia at 24 h, and all four Albulin doses (1–10 mg/kg) lowered ($P < 0.05$) glucose level up to 12 h postinjection.

To evaluate whether currently available short-acting insulin analogs retain the ability to induce hypoglycemia in the presence of Albulin, diabetic mice treated with Albulin (2.5 mg/kg s.c.) were reinjected with Humulin R (5.0 units/kg s.c.). Albulin alone was able to maintain a reduced glucose level for almost 24 h (Fig. 6*B*). As expected, Humulin R alone induced a sharp and fast hypoglycemia (peak ~1 h), after which glucose levels returned to high basal levels within 3 h. When Humulin R was reinjected to mice treated with Albulin, an additional reduction ($P < 0.01$) in glucose levels was observed at 1 h after Humulin injection.

In the next experiment, a glucose challenge was given to fasted diabetic mice to mimic prandial events (Fig. 6*C*). Predictably, Humulin R alone produced significant hypoglycemia when administered just before the glucose challenge in mice. Whereas Albulin alone (Albulin-vehicle) was able to reduce glucose levels for the initial 3 h, it did not significantly enhance glucose clearance after the glucose challenge compared with controls. When mice were injected with Humulin R 3 h after Albulin administration and then immediately challenged with glucose, the combination therapy was able to produce a significant ($P < 0.05$) reduction in glucose compared with mice treated with Albulin alone.

In vivo pharmacokinetics of Albulin. Plasma concentrations after intravenous and subcutaneous dosing of Albulin are presented in Fig. 7*A*. The results of the pharmacokinetic analyses are reported in Table 2. A 1.0 mg/kg dose of Albulin was detectable for the 72-h duration of this study after both intravenous and subcutaneous administration. Albulin appears to be largely confined to the plasma after intravenous injection with a volume of

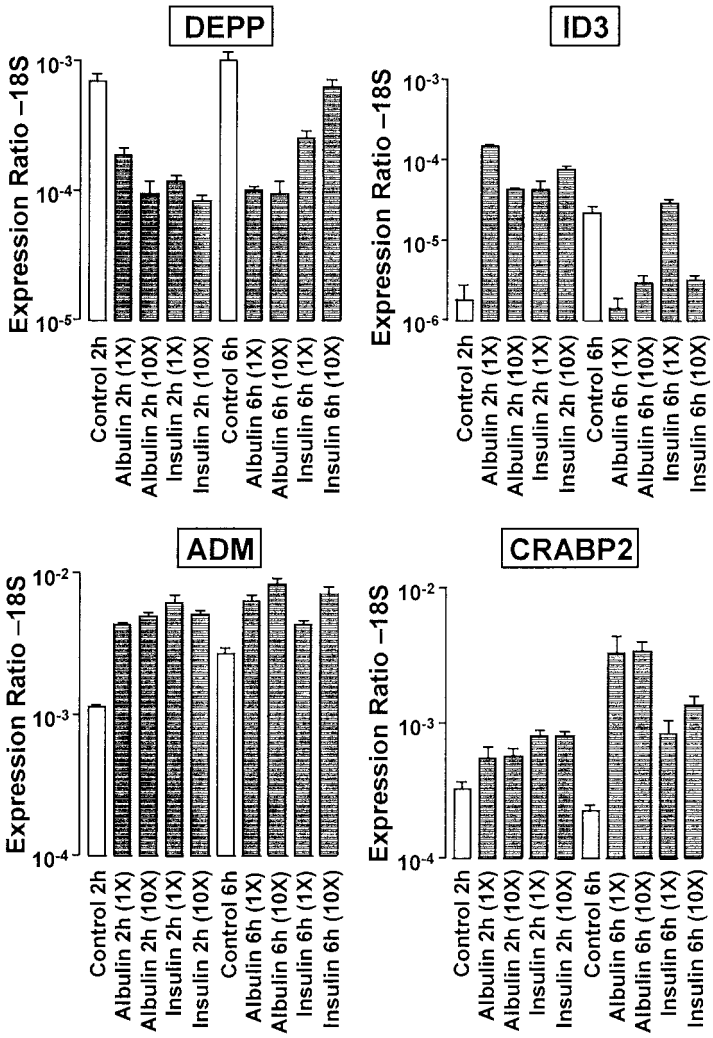

FIG. 5. Confirmation of expression profiles observed in the cDNA array analysis for a subset of genes through qPCR. RNA used in the array study was analyzed through qPCR analysis performed in triplicate to determine steady-state expression levels. mRNA levels were normalized to the level of 18S rRNA.

distribution of 48 ml/kg. Clearance was 4.9 ml · h^{-1} · kg^{-1} after intravenous injection. The apparent volume of distribution was 132 ml/kg after subcutaneous injection, and apparent clearance was 13.5 ml · h^{-1} · kg^{-1}. The increased apparent volume of distribution and apparent clearance values reflect the 36% subcutaneous bioavailability of Albulin relative to intravenous injection. The half-life of Albulin is ~7 h when given intravenously or subcutaneously. The absorption $t_{1/2}$ was 4 h after subcutaneous injection. Research has shown that the interspecies pharmacokinetic behavior of a wide range of therapeutic proteins can be predicted using the equation $Y = aW^b$, where Y is the parameter of interest, a is the allometric coefficient, W is the body weight (in kilograms), and b is the allometric exponent (30). If the 4.9 ml · h^{-1} · kg^{-1} clearance of Albulin observed in a 23-g mouse is scaled (allometric exponent of 0.75) to predict clearance in a 70-kg human, a clearance value of 0.66 ml · h^{-1} · kg^{-1} is obtained. The predicted elimination half-life of Albulin in a 70-kg human would be ~50 h based on scaling of the mouse data (Fig. 7*B*).

DISCUSSION

We report here the characterization of a potent long-acting insulin analog, Albulin, engineered using albumin fusion technology. Others have obtained biologically active single-chain insulins through replacement of proinsulin C-peptide with peptide linkers of various sizes, resulting in a covalent and permanent attachment of the A- and B-chain of insulin (31,32). To determine the influence of single-chain engineering and HSA fusion on the binding characteristics and biological activity of human insulin, Albulin was tested in a range of in vitro assays.

Albulin displayed a lower affinity for the human insulin receptor, as well as a slightly lower affinity for the IGF-I receptor, when compared with human recombinant insulin. Analogs of insulin that result from changes in the native amino acid sequence can display growth-promoting activities higher than those of recombinant human insulin, a characteristic usually attributed to higher affinity for the IGF-I receptor (20,21). The long-acting insulin analog glargine, despite a six- to eightfold increase in IGF-I receptor binding affinity and mitogenic potency (21), has yet to be associated with any mitogenic-related safety issues. Albulin displays a lower affinity for the IGF-I receptor and no more than a threefold increase in growth-promoting activity when compared with recombinant human insulin; it is therefore unlikely to trigger abnormal mitogenic responses in humans.

The two key functions of insulin (i.e., inhibition of gluconeogenesis in the liver and stimulation of glucose uptake in peripheral tissues) were tested in vitro using

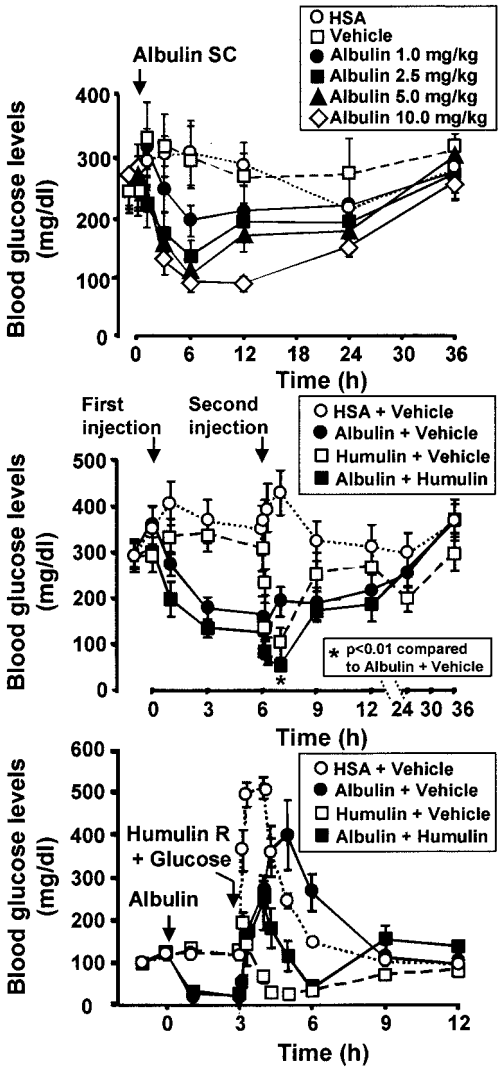

FIG. 6. In vivo control of glycemia by Albulin. *A*: Mean ± SE blood glucose levels after a single subcutaneous injection of vehicle, HSA, and Albulin (1.0, 2.5, 5.0 and 10.0 mg/kg) in STZ-induced diabetic freely fed Balb/cJ mice. Injection of Albulin resulted in the progressive establishment of a hypoglycemic state that was maintained up to 24 h postadministration. *B*: Blood glucose levels after subcutaneous injections of HSA + vehicle, 2.0 mg/kg Albulin + vehicle, vehicle + 5.0 units/kg Humulin R, and 2.0 mg/kg Albulin + 5.0 units/kg Humulin R in freely fed STZ-treated Balb/cJ mice. Treatment of mice with Humulin R after Albulin (Albulin-Humulin) resulted in a further lowering of blood glucose levels at 7 h (*P < 0.001) compared with Albulin alone (Abulin-vehicle). *C*: Blood glucose levels after subcutaneous injections of HSA + vehicle, 2.0 mg/kg Albulin + vehicle, vehicle + 5.0 units/kg Humulin R, and 2.0 mg/kg Albulin + 5.0 units/kg Humulin R in glucose-challenged (oral; 1.2 g/kg) fasted STZ-induced Balb/cJ mice.

Albulin in hepatic and adipose cell lines, respectively. In both systems, Albulin behaved like insulin, with little or no loss of activity. When the regulatory activities of Albulin and insulin on gene transcription were compared using transcription reporter assays, as well as a global gene expression pattern analysis, very few differences were observed between the two proteins.

Pharmacokinetic studies performed in mice can provide information relating to the molecule's pharmacokinetics properties in humans, especially when the data are compared with studies using analogs for which clinical data are available. The elimination half-life of subcutaneously

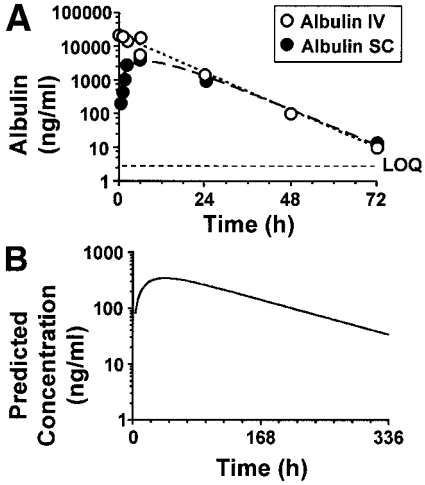

FIG. 7. In vivo pharmacokinetics properties of Albulin. *A*: Predicted and observed concentrations after a single intravenous or subcutaneous injection of Albulin (1 g/kg) in C57Bl/6 mice. The observed concentrations from individual animals are represented by the points, and the predicted concentrations after compartmental analysis are represented by the lines. Data were weighted as $1/C_{pred}^2$ (n = 2 mice/time point). LOQ, limit of quantitation (3.0 ng/ml). *B*: Predicted concentration of Albulin in humans after a single 250-mg/kg dose by subcutaneous injection. The predicted half-life based on allometric scaling of clearance is ~80 h.

administered Albulin in mice was found to be ~7 h. In comparison, the reported elimination half-life of subcutaneously administered recombinant human insulin in mice is ~10 min (33). Based on scaling of the mouse data (30), the predicted elimination half-life of Albulin in a 70-kg human would be ~50 h.

Finally, in in vivo studies, a single subcutaneous injection of Albulin (1–10 mg/kg) was potent enough to induce a dose-dependent progressive reduction of blood glucose levels in severely hyperglycemic STZ-induced diabetic mice. Albulin was able to maintain a near-normoglycemic state for long periods of time while enabling short-acting Humulin R to induce an additional decrease in basal glucose levels. The combination of Albulin and Humulin R was also efficacious in the context of a mealtime increase in glucose levels. These data indicate that Albulin has the

TABLE 2
Pharmacokinetic analyses of Albulin (1.0 mg/kg) in male C57BL/6 mice following intravenous and subcutaneous administration

	Intravenous	Subcutaneous
$AUC_{0-\infty}$ (h · ng · ml^{-1})	203,278 ± 21,297	74,001 ± 12,512
$t_{1/2abs}$ (h)	NA	4.1 ± 1.5
$t_{1/2elim}$ (h)	6.7 ± 0.2	6.8 ± 1.1
CL or CL/F (ml · h^{-1} · kg^{-1})	4.91 ± 0.52	13.51 ± 2.29
t_{max} (h)	NA	7.5 ± 1.0
C_{max} (ng/ml)	20,936 ± 2,593	3,519.6 ± 525.7
MRT (h)	9.7 ± 0.3	15.6*
V or V/F (ml/kg)	48 ± 6	132 ± 41
Bioavailability (%)	36	

Data are estimates ± SE. *Calculated as 1/absorption rate + 1/elimination rate. $AUC_{0-\infty}$, area under the plasma concentration curve extrapolated to infinity; $t_{1/2abs}$, absorption half-life; $t_{1/2elim}$, elimination half-life; CL, total clearance; CL/F, apparent clearance after extravascular administration; t_{max}, time to maximal plasma concentration; C_{max}, maximal plasma concentration; MRT, mean residence time; V, volume of distribution; V/F, apparent volume of distribution after extravascular administration; NA, not applicable.

promise to be used in a dual-therapy setting with short-acting insulin analogs.

In conclusion, we have engineered a long-acting insulin analog, Albulin, using albumin-fusion technology. Albulin displays improved in vivo pharmacokinetic and pharmacodynamic profiles while retaining the in vitro potency of recombinant human insulin. Albulin has shown to have the potential as a therapeutic option for the maintenance of long-term, near-normoglycemia for the treatment of diabetes.

ACKNOWLEDGMENTS

We thank Drs. Robert Melder, Vikram Patel, and David Hilbert for their help with the manuscript preparation.

REFERENCES

1. Bolli GB: Clinical strategies for controlling peaks and valleys: type 1 diabetes. *Int J Clin Pract Suppl* 129:65–74, 2002
2. Yki-Jarvinen H: Combination therapy with insulin and oral agents: optimizing glycemic control in patients with type 2 diabetes mellitus. *Diabetes Metab Res Rev Suppl* 3:S77–S81, 2002
3. Owens D, Zinman B, Bolli GB: Insulins today and beyond. *Lancet* 358:739–746, 2001
4. Vajo Z, Fawcett J, Duckworth WC: Recombinant DNA technology in the treatment of diabetes: insulin analogs. *Endocr Rev* 22:706–717, 2001
5. Lepore M, Pampanelli S, Fanelli C, Porcellati F, Bartocci L, Di Vincenzo A, Cordoni C, Costa E, Brunetti P, Bolli GB: Pharmacokinetics and pharmacodynamics of subcutaneous injection of long-acting human insulin analog glargine, NPH insulin, and ultralente human insulin and continuous subcutaneous infusion of insulin lispro. *Diabetes* 49:2142–2148, 2000
6. McKeage K, Goa KL: Insulin glargine: a review of its therapeutic use as a long-acting agent for the management of type 1 and 2 diabetes mellitus. *Drugs* 61:1599–1624, 2002
7. Kurtzhals P, Havelund S, Jonassen I, Kiehr B, Larsen UD, Ribel U, Markussen J: Albumin binding of insulins acylated with fatty acids: characterization of the ligand-protein interaction and correlation between binding affinity and timing of the insulin effect in vivo. *J Biochem* 312:725–731, 1995
8. King AB, Armstrong D: A comparison of basal insulin delivery: continuous subcutaneous insulin infusion versus glargine (Letter). *Diabetes Care* 26:1322, 2003
9. Ratner RE, Hirsch IB, Neifing JL, Garg SK, Mecca TE, Wilson CA: Less hypoglycemia with insulin glargine in intensive insulin therapy for type 1 diabetes: U.S. Study Group of Insulin Glargine in Type 1 Diabetes. *Diabetes Care* 23:639–643, 2000
10. Vajo Z, Duckworth WC: Genetically engineered insulin analogs: diabetes in the new millenium. *Pharmacol Rev* 52:1–9, 2000
11. Osborn BL, Sekut L, Corcoran M, Poortman C, Sturm B, Chen G, Mather D, Lin HL, Parry TJ: Albutropin: a growth hormone-albumin fusion with improved pharmacokinetics and pharmacodynamics in rats and monkeys. *Eur J Pharmacol* 456:149–158, 2002
12. Sung C, Nardelli B, LaFleur DW, Blatter E, Corcoran M, Olsen HS, Birse CE, Pickeral OK, Zhang J, Shah D, Moody G, Gentz S, Beebe L, Moore PA: An IFN-beta-albumin fusion protein that displays improved pharmacokinetic and pharmacodynamic properties in nonhuman primates. *J Interferon Cytokine Res* 23:25–36, 2003
13. Reed BC, Lane MD: Insulin receptor synthesis and turnover in differentiating 3T3–L1 preadipocytes. *Proc Natl Acad Sci U S A* 77:285–289, 1980
14. Egan JM, Montrose-Rafizadeh C, Wang Y, Bernier M, Roth J: Glucagon-like peptide-1(7–36) amide (GLP-1) enhances insulin-stimulated glucose metabolism in 3T3–L1 adipocytes: one of several potential extrapancreatic sites of GLP-1 action. *Endocrinology* 135:2070–2075, 1994
15. Wang JC, Stafford JM, Scott DK, Sutherland C, Granner DK: The molecular physiology of hepatic nuclear factor 3 in the regulation of gluconeogenesis. *J Biochem* 275:14717–14721, 2000
16. Kjeldsen T: Yeast secretory expression of insulin precursors. *Appl Microbiol Biotechnol* 54:277–286, 2000
17. Nilsson J, Jonasson P, Samuelsson E, Stahl S, Uhlen M: Integrated production of human insulin and its C-peptide. *J Biotechnol* 48:241–250, 1996
18. Jonasson P, Nilsson J, Samuelsson E, Moks T, Stahl S, Uhlen M: Single-step trypsin cleavage of a fusion protein to obtain human insulin and its C peptide. *Eur J Biochem* 236:656–661, 1996
19. Jehle PM, Lutz MP, Fussgaenger RD: High affinity binding sites for proinsulin in human IM-9 lymphoblasts. *Diabetologia* 39:421–432, 1996
20. De Meyts P: The structural basis of insulin and insulin-like growth factor-I receptor binding and negative co-operativity, and its relevance to mitogenic versus metabolic signalling. *Diabetologia* 37:S135–S148, 1994
21. Kurtzhals P, Schaffer L, Sorensen A, Kristensen C, Jonassen I, Schmid C, Trub T: Correlations of receptor binding and metabolic and mitogenic potencies of insulin analogs designed for clinical use. *Diabetes* 49:999–1005, 2000
22. Hansen BF, Danielsen GM, Drejer K, Sorensen AR, Wiberg FC, Klein HH, Lundemose AG: Sustained signaling from the insulin receptor after stimulation with insulin analogs exhibiting increased mitogenic potency. *J Biochem* 315:271–279, 1996
23. Napier JR, Thomas MF, Sharma M, Hodgkinson SC, Bass JJ: Insulin-like growth factor-1 protects myoblasts from apoptosis but requires other factors to stimulate proliferation. *J Endocrinol* 163:63–68, 1999
24. Saltiel AL, Kahn RC: Insulin signaling and the regulation of glucose and lipid metabolism. *Nature* 414:799–806, 2001
25. O'Brien RM, Streeper RS, Ayala JE, Stadelmaier BT, Hornbuckle LA: Insulin-regulated gene expression. *Biochem Soc Trans* 29:552–558, 2001
26. Sutherland C, O'Brien RA, Granner DK: New connections in the regulation of PEPCK gene expression by insulin. *Philos Trans R Soc Lond B Biol Sci* 351:191–199, 1996
27. Horton JD, Goldstein JL, Brown MS: SREBPs: activators of the complete program of cholesterol and fatty acid synthesis in the liver. *J Clin Invest* 109:1125–1131, 2002
28. Barroso I, Santisteban P: Insulin-induced early growth response gene (Egr-1) mediates a short-term repression of rat malic enzyme gene transcription. *J Biochem* 274:17997–18004, 1999
29. Eisen MB, Spellman PT, Brown PO, Botstein D: Cluster analysis and display of genome-wide expression patterns. *Proc Natl Acad Sci U S A* 95:14863–14868, 1998
30. Mordenti J, Chen SA, Moore JA, Ferraiolo BL, Green JD: Interspecies scaling of clearance and volume of distribution data for five therapeutic proteins. *Pharm Res* 8:1351–1359, 1991
31. Kristensen C, Andersen AS, Hach M, Wiberg FC, Schaffer L, Kjeldsen T: A single-chain insulin-like growth factor I/insulin hybrid binds with high affinity to the insulin receptor. *J Biochem* 305:981–986, 1995
32. Lee HC, Kim SJ, Kim KS, Shin HC, Yoon JW: Remission in models of type 1 diabetes by gene therapy using a single-chain insulin analogue. *Nature* 408:483–488, 2000
33. Cresto JC, Lavine RL, Buchly ML, Penhos JC, Bhathena SJ, Recant L: Half life of injected 125I-insulin in control and ob/ob mice. *Acta Physiol Lat Am* 27:7–15, 1977